FULL PAPER

Open Access

Deep groundwater discharge after the 2011 Mw 6.6 Iwaki earthquake, Japan

Tsutomu Sato[*], Kohei Kazahaya, Norio Matsumoto and Masaaki Takahashi

Abstract

Hot spring discharge was linked to the 2011 Mw 6.6 Iwaki earthquake. Periodic surveys revealed that the discharge continued for more than 7 years, which is a rare and valuable long-term record of hot spring discharge triggered by an earthquake in a non-volcanic area. In terms of coseismic changes, based on a comparison of the spatial distribution of changes in the coseismic water head and calculated crustal volumetric strain using a fault model, hot spring water discharge was found to be caused by a change in the coseismic crustal volumetric strain. As for the postseismic changes, observations over 7 years revealed a gradual rise in the temperature and chloride ion concentration of the hot spring water. Such long-term hot spring discharge may be explained by the following two causes: the rise of thermal water from the deep part and the permeability changes along the hot spring channels.

Keywords: Coseismic hydrological change, Hot spring water discharge, 2011 Iwaki earthquake, 2011 Tohoku-oki earthquake, Crustal strain, Water temperature, Chloride ion, Sulfate ion, Oxygen stable isotopic ratio

Introduction

The phenomenon of hot spring water flows being renewed after an earthquake has been documented in several regions (Hosono et al. 2018; Manga and Rowland 2009; Okuyama et al. 2016; Wang et al. 2004a). The Matsushiro earthquake swarm, which occurred from 1965 to 1967, caused the discharge of high-salinity hot spring water ($Cl^- > 2000$ mg/L) that continued even into 2011, i.e., for a span of 46 years (Okuyama et al. 2016). After the 2016 Kumamoto earthquake, groundwater discharge is thought to have been a direct result of volcanic activity and continued for over one year (Hosono et al. 2018). Such long-term (i.e., more than a year) hot spring water and groundwater discharge occasionally occur in volcanic areas (Hosono et al. 2018; Okuyama et al. 2016). This is because volcanic fluid rises in volcanic areas, in which underground hot spring water reservoirs characterized by high pressure are likely to exist.

Concerning the mechanism that allows hot spring water to continue to discharge after an earthquake,

previous studies have proposed a connection between a high-pressure reservoir and the surface because of the occurrence of cracks formed by the earthquake (Sibson and Rowland 2003; Wang et al. 2004a). Previous studies have further attempted to clarify the relationship between volcanic activity and hot spring discharge based on geochemical analyses of this water (Giammanco et al. 2008; Hosono et al. 2018; Nishio et al. 2010). For example, the long-term discharge of hot spring water as a result of the Matsushiro earthquake may be related to volcanic activity (Okuyama et al. 2016). On the other hand, Nakamura (1971) distinguished this phenomenon from general volcanic activity and described it as "water eruptions".

Multiple-year prolongation of hot spring water and groundwater anomalies associated with earthquakes in non-volcanic areas is rare. Hot spring water levels have reportedly risen abnormally for 9 years at Dogo hot spring where is located on a specific fault zone in Japan (Koizumi and Kinoshita 2017), but such multiple-year-long anomalous discharge of hot spring water and groundwater has rarely been reported. Hot spring water and groundwater discharge often occur along with earthquakes, but the discharge period is limited. In most cases,

*Correspondence: sugar@ni.aist.go.jp
Geological Survey of Japan, AIST, 1-1-1 Higashi, Tsukuba, Ibaraki 305-8567, Japan

Sato *et al. Earth, Planets and Space*   (2020) 72:54

Page 2 of 11

including changes in river flow attributable to groundwater discharge, the amount of discharge starts diminishing several months after the earthquake, usually stopping after several years (Rojstaczer and Wolf 1992; Sato et al. 2000; Manga and Rowland 2009; Wang et al. 2004b; Wang and Manga 2015). Such hot spring water and groundwater discharges may have various causes, including liquefaction, changes in crustal strain, and changes in aquifer permeability (Manga and Wang 2015). High-pressure hot spring water reservoirs in non-volcanic areas exist within narrow boundaries, such as areas where the crust is pressured by tectonic activity due to plate or fault movement (Oki et al. 1999; Roberts et al. 1996). Therefore, it is plausible for hot spring water and groundwater to continue to discharge for more than a year even in non-volcanic areas.

Iwaki is a non-volcanic area, but hot spring water with a temperature of over 50 °C can be pumped to the surface (Nakamura 1909, 1959; Nakamura and Ando 1953). The Joban area, adjacent to the south of Iwaki, contains hot springs with temperatures of over 70 °C, whose origin is thought to be water generated by dehydration of a plate boundary at a depth of 50 km (Togo et al. 2014). Additionally, seismic velocity tomography has revealed a low-velocity zone at a depth of 40 km in Iwaki, suggesting the existence of an extensive deep groundwater reservoir (Tong et al. 2012).

On March 11, 2011, the Tohoku-oki earthquake (Mw 9.0) occurred off the northeastern coast of Japan (Fig. 1a). The Iwaki earthquake (Mw 6.6) occurred 1 month later (April 11, 2011) and has been linked to the Tohoku-oki earthquake (Muto et al. 2014; Okada et al. 2011). After the Iwaki earthquake, hot spring water was discharged at several sites in the Iwaki area, and the discharge has continued for more than 7 years. Such long-term discharge in non-volcanic areas has not previously been reported. In this study, we clarified the temporal changes in hot spring water discharge, analyzed the major chemical composition and oxygen stable isotopic ratio of the water, and discussed the mechanism of hot spring water discharge continuing for such long periods in non-volcanic areas.

Geological setting and 2011 Iwaki earthquake

Iwaki is located in the Tohoku region of Japan along the Pacific coast, where there are no Quaternary volcanoes (Fig. 1a). The basement is composed of Cretaceous granitic rocks covered by a Tertiary sedimentary layer (Sugai et al. 1957) (Fig. 1b) with a northwest–southeast strike and a dip angle of 10–20° to the east (Suto et al. 2005). The lower part of the sedimentary layer contains coal beds, which supported coal mines operational until 1976 (Ohara 1996). In addition, the sedimentary

layer can be divided into several blocks cut by a south-trending normal fault with an east–west strike. The Karasudate fault caused the formation of a vertical step of approximately 300 m in the sedimentary layer, especially in the area shown by the cross-section in Fig. 1b (Sugai et al. 1957).

The Iwaki earthquake occurred at a depth of 6 km in Iwaki City, Fukushima Prefecture (Fukushima et al. 2013) (Fig. 1a). As a result, surface displacements ranging from several tens of centimeters to 2 m were observed along two normal faults (namely the Itozawa and Yunodake faults) (Mizoguchi et al. 2012; Toda and Tsutsumi 2013). Based on Global Navigation Satellite System (GNSS) observations from the Geospatial Information Authority of Japan, large changes were observed in the baseline length (between Iwaki and Iwaki 2 in Fig. 1a). The amplitudes dilated by 8 cm during the Tohoku-oki earthquake and contracted by 16 cm during the Iwaki earthquake (Geospatial Information Authority of Japan 2011) (Fig. 1c).

Hot springs in Iwaki

In the Iwaki area, hot spring water flowed to the ground surface until 100 years ago. According to Nakamura (1909), when hot spring wells began to be excavated, hot spring water flowed out into the vicinity of Yumoto at a rate of 14 L/s (Fig. 1). Large-scale coal mine development began at the beginning of the 1900s, enabling the study of hot spring discharge into mining tunnels (Arakawa 1961; Nakamura 1959; Nakamura and Ando 1953). According to these studies, a north–south-striking fault was the main cause of hot spring water inflow into the mines. Additionally, the temperature and quality of the hot spring water exhibited differences depending on the discharge depth. An analysis of the characteristics of the hot spring water discharged into shallow areas (i.e., above a depth of 400 m) showed that the temperature and Cl^- concentration were relatively low (20–40 °C and < 500 mg/L, respectively), and the SO_4^{2-} concentration was relatively high (> 1500 mg/L) (Nakamura and Ando 1953). On the other hand, the characteristics of the hot spring water discharged in deeper parts of the mine (600–700 m) exhibited a relatively high temperature (50–60 °C), low SO_4^{2-} concentration (< 500 mg/L), and high Cl^- concentration (> 1000 mg/L).

Previous studies suggested that hot spring water in the Iwaki area has a fossil seawater origin based on an I^-/Cl^- ratio that is higher than that of seawater (Arakawa 1961; Nakamura 1959). Togo et al. (2014) analyzed the hot spring water in and around the Iwaki area to obtain its hydrogen and oxygen stable isotope, radioactive iodine and chlorine isotope, and tritium compositions. The results suggested that the origin of the hot spring water

Sato *et al. Earth, Planets and Space*   (2020) 72:54

Page 3 of 11
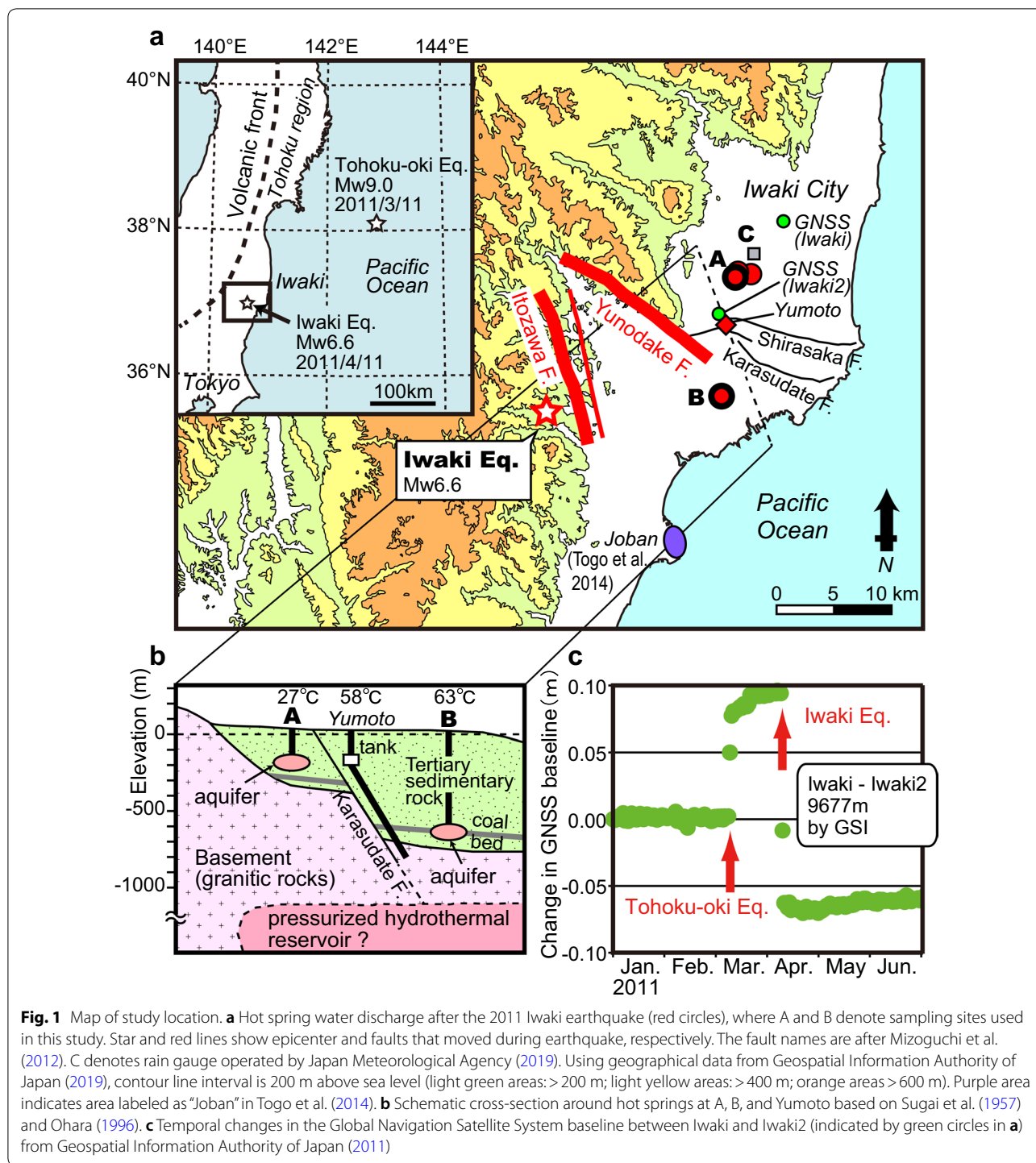
Fig. 1 Map of study location. **a** Hot spring water discharge after the 2011 Iwaki earthquake (red circles), where A and B denote sampling sites used in this study. Star and red lines show epicenter and faults that moved during earthquake, respectively. The fault names are after Mizoguchi et al. (2012). C denotes rain gauge operated by Japan Meteorological Agency (2019). Using geographical data from Geospatial Information Authority of Japan (2019), contour line interval is 200 m above sea level (light green areas: > 200 m; light yellow areas: > 400 m; orange areas > 600 m). Purple area indicates area labeled as "Joban" in Togo et al. (2014). **b** Schematic cross-section around hot springs at A, B, and Yumoto based on Sugai et al. (1957) and Ohara (1996). **c** Temporal changes in the Global Navigation Satellite System baseline between Iwaki and Iwaki2 (indicated by green circles in **a**) from Geospatial Information Authority of Japan (2011)

is related to diagenetic fluid released by the 50-km-deep plate boundary. Additionally, using radioactive iodine dating, they estimated that the ascent of hydrothermal fluid was 2–5 mm/year.

Materials and methods

After the 2011 Iwaki earthquake, hot spring water discharge was confirmed at four sites in Iwaki City (red circles in Fig. 1a). We began surveying the discharge once every 1–3 months at two sites, namely sites A and B.

Sato *et al. Earth, Planets and Space*   (2020) 72:54

Page 4 of 11

The surveys at sites A and B began 17 and 37 days after the earthquake, respectively. We used the total amount method to measure the flow rate at site A and the float method at site B. The total amount method is a procedure whereby discharged water is collected in a bag and the discharged rate is calculated from the discharge volume and time. The float method consists of calculating the discharge rate using the cross-sectional area of the flow path and surface flow velocity.

We measured the water temperature, pH, and electrical conductivity in the field at both sites using a thermometer (Ebro TFX 410, Xylem Analytics UK Ltd.) and a pH–electrical conductivity meter (LAQUA D-74, HORIBA, Ltd.), respectively. Hot spring water was collected using polyethylene bottles, and the concentrations of the major chemical compositions and the oxygen stable isotopic ratios ($\delta^{18}O$) were immediately analyzed in our laboratory. The concentrations of the major chemical compositions were analyzed using ion chromatography (ICS-2100, Thermo Fisher Scientific Inc.), and the $\delta^{18}O$ was analyzed via mass spectrometry (Delta Plus, Thermo

Fisher Scientific Inc.) and a Cavity Ringdown Spectrometer (L2120-i, Picarro Inc.).

Spatial coseismic groundwater level changes in Iwaki City

To investigate the hydrological impact of the 2011 Iwaki earthquake, we surveyed the water head changes in the hot springs in the Iwaki area. As shown in Fig. 2, the water level increased in three hot springs (red triangles) in addition to the four sites (red circles) characterized by discharge. On the other hand, we observed a decrease in the water level at two hot springs (blue triangles in Fig. 2). Subsequent surveys revealed that the water heads returned to their original levels within 1 year after the earthquake except at Yumoto and the four sites where discharge occurred. These results are summarized in Table 1.

To investigate the relationship between regional crustal deformation and water head changes due to the earthquake, we calculated the distribution of the change in crustal volumetric strain using a fault model. The fault parameters were estimated from the analytical results
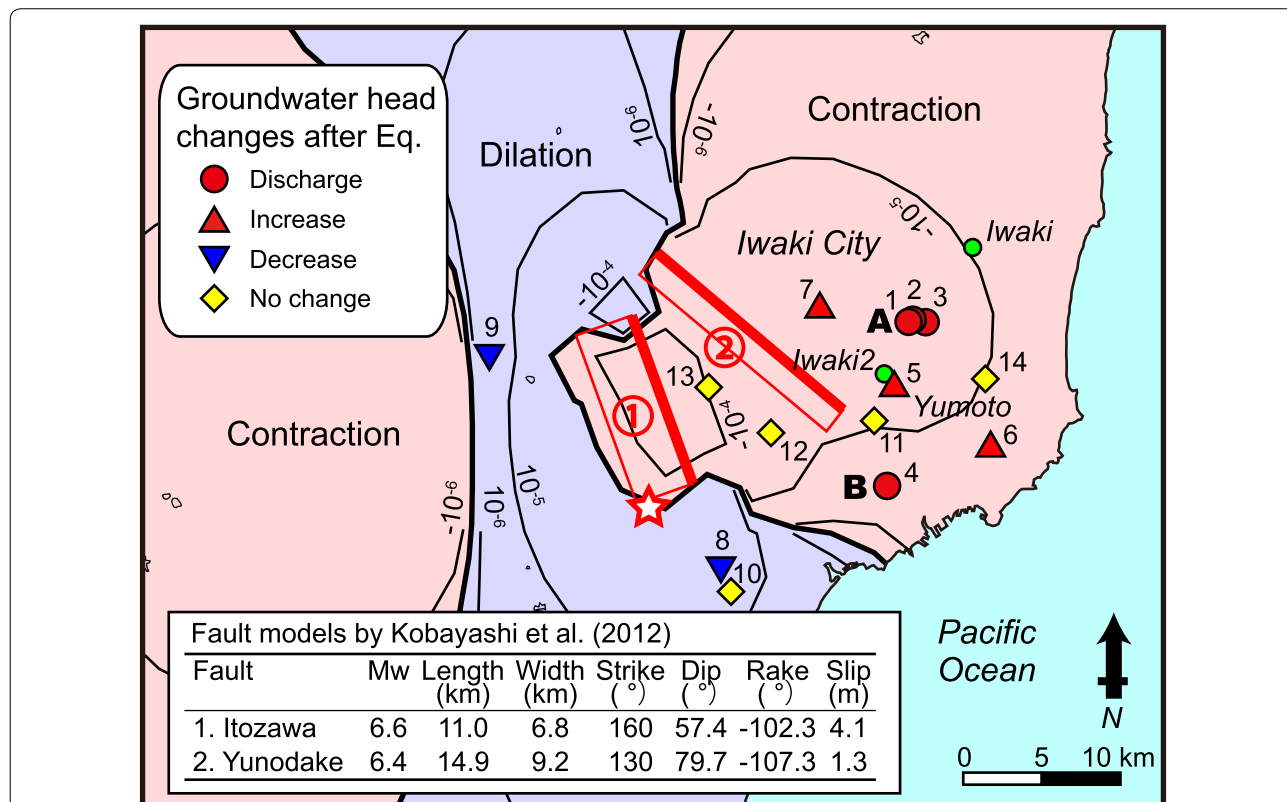
Fig. 2 Spatial distribution of coseismic changes in the groundwater head due to 2011 Iwaki earthquake based on field survey. Red circles, red triangles and blue triangles indicate hot springs where discharge, water level increase, and water level decrease were observed during earthquake, respectively, and numbers correspond to those in Table 1. Calculated results of the changes in the crustal volumetric strain during earthquake using fault models proposed in Kobayashi et al. (2012) are also shown

Fault models by Kobayashi et al. (2012)

Fault	Mw	Length (km)	Width (km)	Strike (°)	Dip (°)	Rake (°)	Slip (m)
1. Itozawa	6.6	11.0	6.8	160	57.4	-102.3	4.1
2. Yunodake	6.4	14.9	9.2	130	79.7	-107.3	1.3

Sato *et al. Earth, Planets and Space* (2020) 72:54

Page 5 of 11

Table 1 Results of interview survey for coseismic change of the 2011 Iwaki earthquake and measurement and analysis results for hot spring water around the Iwaki area

No.	Location	Visit date	Coseismic change at Iwaki Eq.	Temp. (°C)	HCO_3^- (mg/L)	Cl^- (mg/L)	SO_4^{2-} (mg/L)	$\delta^{18}O$ (‰)
1	Uchigo-takasakamachi1 (A)	28 Apr. 2011	Discharge	26.9	267	88.9	475	− 7.7
2	Uchigo-takasakamachi2	19 Jun. 2014	Discharge	27.8	229	87.8	508	− 7.8
3	Mimayamachi	22 Jun. 2011	Discharge	25.6	311	76.8	527	− 7.6
4	Izumi-tamatsuyu (B)	18 May 2011	Discharge	56.1	190	1360	51.9	− 6.9
5	Yumoto	28 Apr. 2011	Water level increase	58.3	107	702	377	− 7.4
6	Onahama	28 Apr. 2011	Water level increase	14.0	312	216	239	− 7.4
7	Uchigo-kouyamachi	28 Apr. 2011	Water level increase	15.8	189	3.5	12.9	− 8.1
8	Kawabemachi	20 Apr. 2011	Water level decrease	10.6	223	4.4	19.5	− 7.6
9	Furudonomachi	18 May 2011	Water level decrease	10.8	127	20.5	12.4	− 9.9
10	Nakosomachi	20 Apr. 2011	No change	12.3	54.9	12.5	14.6	− 7.6
11	Joban-shiratorimachi	6 Jun. 2011	No change	31.6	0.0	64.5	169	− 7.5
12	Toonomachi-taki	6 Jun. 2011	No change	17.9	130	6.0	52.3	− 7.6
13	Toonomachi-oodaira	20 Apr. 2011	No change	–	–	–	–	–
14	Taira-yoshinoya	22 Sep. 2011	No change	–	–	–	–	–

"No." corresponds to the number in Fig. 2

of crustal movement observed using interferometric synthetic-aperture radar (Kobayashi et al. 2012). These parameters were input into the MICAP-G program (Naito and Yoshikawa 1999; Okada 1992) to analyze crustal deformation and calculate the coseismic changes in crustal volumetric strain distribution associated with the 2011 Iwaki earthquake. A comparison of these results with the distribution of water head changes indicated a rise in the water head in the area expected to exhibit changes in contraction crustal strain (Fig. 2). In areas expected to exhibit changes in dilatation crustal strain, a drop in water head occurred. Therefore, we suggest that changes in the crustal volumetric strain caused the coseismic water-head changes in the hot springs.

At Yumoto, hot spring water levels were measured approximately once a day prior to the earthquake (Joban Yumoto Onsen Co., Ltd., personal communication). According to the observations, a drop in the water level of 10 m occurred during the Tohoku-oki earthquake, and an increase of 20 m occurred during the Iwaki earthquake. As mentioned above, a dilatation of 8 cm was observed during the Tohoku-oki earthquake, whereas a contraction of 16 cm was observed during the Iwaki earthquake based on the Global Navigation Satellite System baseline length of 9877 m between Iwaki and Iwaki 2 (Fig. 1c) around Yumoto (Geospatial Information Authority of Japan 2011). Thus, the linear strain change in the northeast–southwest direction near Yumoto during the Tohoku-oki earthquake was 8.1 μ-strain. Therefore, the sensitivity of the water level change at the Yumoto hot spring to the linear strain was calculated as

− 1.2 m/μ-strain. Using this sensitivity, the water level during the Iwaki earthquake was expected to increase by 20 m, which is consistent with the observed water level change. Therefore, we suggest that changes in the coseismic crustal volumetric strain caused changes in the water level during the earthquakes.

Hot spring chemical characteristics at sites A and B

Figure 3 shows that the hot spring water at site A had a SO_4^{2-}-rich composition, whereas site B had a Cl^--rich composition. As mentioned above, the hot spring at the coal mine in Iwaki had SO_4^{2-}-rich shallow portions with a low temperature, whereas deeper portions had a high temperature and were Cl^--rich (Arakawa 1961; Nakamura 1959; Nakamura and Ando 1953). Stiff diagrams (Fig. 3) display the major chemical composition of the hot spring water discharged into the coal mine beneath sites A and B (Ohara 1996). By comparing the shapes of the Stiff diagrams, we observed that both the shapes of A and B were similar to that of the hot spring water discharged beneath sites A and B, respectively. However, the concentration of the major chemical compositions was halved. For example, the SO_4^{2-} concentration of A was less than half of that of the hot spring water beneath site A, and the Cl^- concentration of site B was less than half of that of the hot spring water beneath site B. Therefore, we suggest that as the hot spring water at the coal mine beneath sites A and B rose toward the respective ground surfaces, it continuously mixed with groundwater shallower than that of each coal mines.
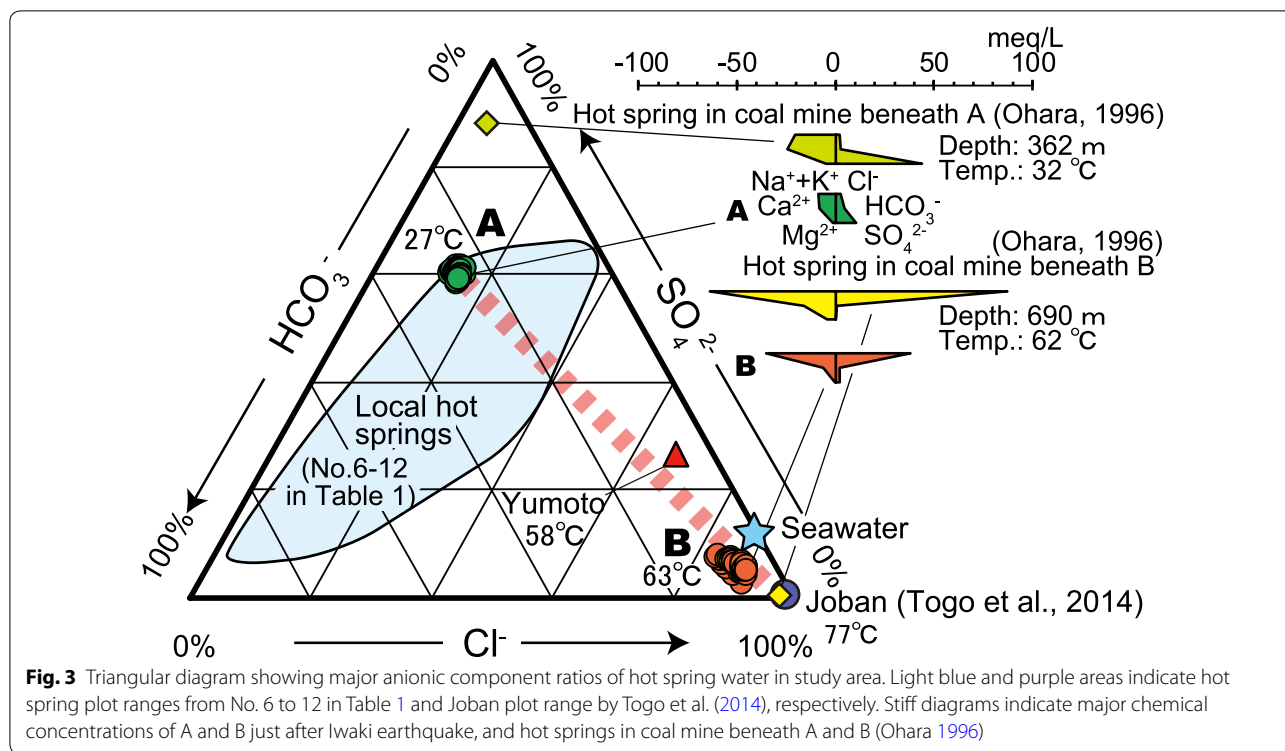
Sato *et al. Earth, Planets and Space*   (2020) 72:54

Page 6 of 11

Fig. 3 Triangular diagram showing major anionic component ratios of hot spring water in study area. Light blue and purple areas indicate hot spring plot ranges from No. 6 to 12 in Table 1 and Joban plot range by Togo et al. (2014), respectively. Stiff diagrams indicate major chemical concentrations of A and B just after Iwaki earthquake, and hot springs in coal mine beneath A and B (Ohara 1996)

Figure 3 shows the major anionic component ratios of hot spring waters at Yumoto and Joban in addition to those sites A and B (Togo et al. 2014). The order of hot spring water temperature is as follows: Joban > B > Yumoto > A. This order also corresponded to that for the ratio of the Cl^- concentration to the total major anion composition. This trend is also shown in Fig. 4, which depicts the relationship between the Cl^- concentration and $\delta^{18}O$. The thick dotted line in Fig. 4 extended to a $\delta^{18}O$ of zero corresponds to a Cl^- concentration of approximately 13,000 mg/L, not reaching a concentration of 19,000 mg/L, which is the value of general seawater. Thus, we speculate that the origin of the hot spring water was not fossil seawater, but diagenetic fluids whose Cl^- concentrations water reduced due to influences from dehydration reactions in the surrounding rocks.

Temporal changes at site A

Figure 5 shows the observational results from 2011 to 2018 for the flow rate, water temperature, and Cl^- and SO_4^{2-} concentrations at sites A and B. This figure also shows the daily precipitation and a precipitation index that accounts for the accumulated precipitation at site C (Fig. 1). The precipitation index was obtained so that the increase or decrease in precipitation in a particular year or season can be easily understood. Specifically, this index was calculated by subtracting the integrated value

of the average daily precipitation from the accumulated daily precipitation. The average daily precipitation was calculated using data from the 7 years after the earthquake, and the precipitation data were based on data from the Japan Meteorological Agency (2019).

The flow rate at site A increased from 2.1 L/s after the earthquake to 4.7 L/s over 5 months, which was maintained until 2018. The period from 2011 to 2015 was characterized by 1- to 2-year cycles with ranges fluctuating by about 2 L/s. The total discharge volume at site A reached 1 billion liters over 7 years since the earthquake occurred until 2018. Periodic changes in the flow rate at site A were correlated with the precipitation index. This implies that pressure increases in shallow groundwater during precipitation events strongly affected the flow rate.

The water temperature at site A was 27.0 °C immediately after the earthquake, which tended to rise, reaching 27.8 °C in 2018 (Fig. 5a). The average rate of temperature increase was approximately 0.1 °C/year during this period. The Cl^- concentration at site A decreased from 2.5 meq/L immediately after the earthquake to 2.2 meq/L in the 6 months following the earthquake and then increased to 2.6 meq/L in the following 8 months (Fig. 5b). Subsequent increases or decreases occurred within a ± 0.2 meq/L range. The SO_4^{2-} concentrations increased from 9.9 meq/L immediately after

Sato *et al. Earth, Planets and Space*   (2020) 72:54

Page 7 of 11
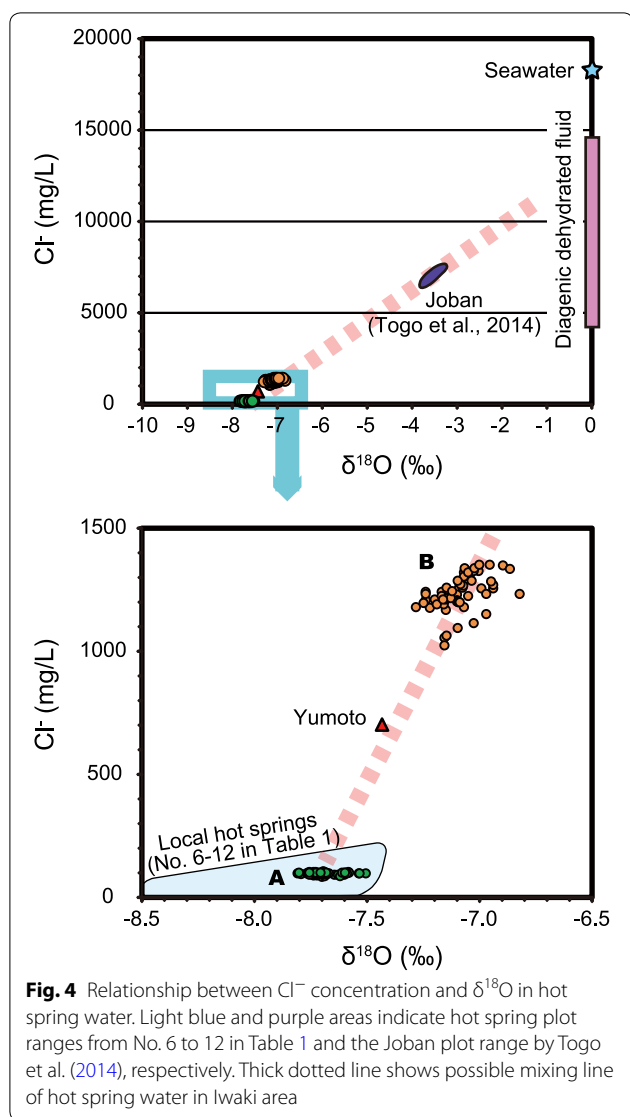
Fig. 4 Relationship between Cl⁻ concentration and $\delta^{18}O$ in hot spring water. Light blue and purple areas indicate hot spring plot ranges from No. 6 to 12 in Table 1 and the Joban plot range by Togo et al. (2014), respectively. Thick dotted line shows possible mixing line of hot spring water in Iwaki area

the earthquake to 11.5 meq/L within 1 year. Subsequent increases or decreases occurred within a ± 0.6 meq/L range.

The Cl⁻ and SO_4^{2-} concentrations at site A were correlated, such that changes in the patterns were similar, especially after 2014 (Fig. 5b). Moreover, as illustrated in plot A in Fig. 3, the major anion composition ratio remained located at practically the same place, there were almost no temporal changes in the anion composition ratios. Therefore, the temporal changes in the Cl⁻ and SO_4^{2-} concentrations at site A (Fig. 5b) after 2014 may have occurred because of mixing with shallow groundwater with a low concentration of dissolved components. This supports the notion that hot spring water at site A formed due to mixing between deep hot spring water discharged into the coal mine beneath site A and shallow groundwater (Fig. 3).

For the first 6 months following the earthquake, we observed a decrease in SO_4^{2-} and an increase in Cl⁻ concentration at site A (Fig. 5b); this change is illustrated in Fig. 6. During the Iwaki earthquake, hot spring water discharges occurred near Yumoto due to changes in crustal strain contraction (Fig. 6a). At this time, the discharged groundwater is thought to have been stagnant groundwater along the groundwater flow path between the ground surface and hot spring water aquifer at site A. The Cl⁻ concentration of this stagnant water was as high as 2.5 meq/L, but the reason for this is unknown. Subsequently, the SO_4^{2-}-rich hot spring water at a depth of 300 m reached the ground surface, leading to an increased mixing ratio and gradual increase in SO_4^{2-} concentration in the discharged water (Fig. 6b). Finally, it is thought that the aquifer pressure was maintained due to the influence of rising hot spring water (Fig. 6c). Figure 5b shows that the SO_4^{2-} concentration decreased slightly after 2013, whereas the Cl⁻ concentration increased slightly. Since the concentration change was small, it did not appear as a change in the plot in Figs. 3 and 4.

The depth of the aquifer at site A was approximately 200 m based on the local geothermal gradient (9 °C/100 m; Nakamura and Ando 1953) and mean annual temperature of approximately 13 °C in Iwaki City (Japan Meteorological Agency 2019). This depth was shallower than that of the coal bed at 300 m (Ohara 1996) beneath site A.

Temporal changes at site B

The flow rate at site B gradually decreased from 95 L/s immediately after the earthquake to approximately 40 L/s in 2018 (Fig. 5c). The total flow volume for 7 years after the earthquake until 2018 reached 15 billion liters. The flow rate change was characterized by a changing 1- to 2-year cycle, with a fluctuation range of approximately 20 L/s (Fig. 5c). The water temperature at site B was 56.0 °C immediately after the earthquake and increased to 63.0 °C in 1 year (Fig. 5c). From mid-2012 to 2016, the water temperature gradually increased by 1.8 °C to 64.8 °C. The rate of increase in water temperature during this period was 0.36 °C/year. The water temperature after 2017 was nearly constant.

The Cl⁻ concentration of hot spring water at site B decreased from 38 meq/L immediately after the earthquake to 29 meq/L in the following 6 months and then increased to 35 meq/L after another 4 months (Fig. 5d). After 2012, the Cl⁻ concentration slightly increased, reaching 38 meq/L by 2018. The rate of increase for the Cl⁻ concentration during this period was 0.4 meq/L/year. The SO_4^{2-} concentration increased from 1.0 meq/L after the earthquake to 2.5 meq/L in 1 year. Since then, the

Sato *et al. Earth, Planets and Space* (2020) 72:54

Page 8 of 11
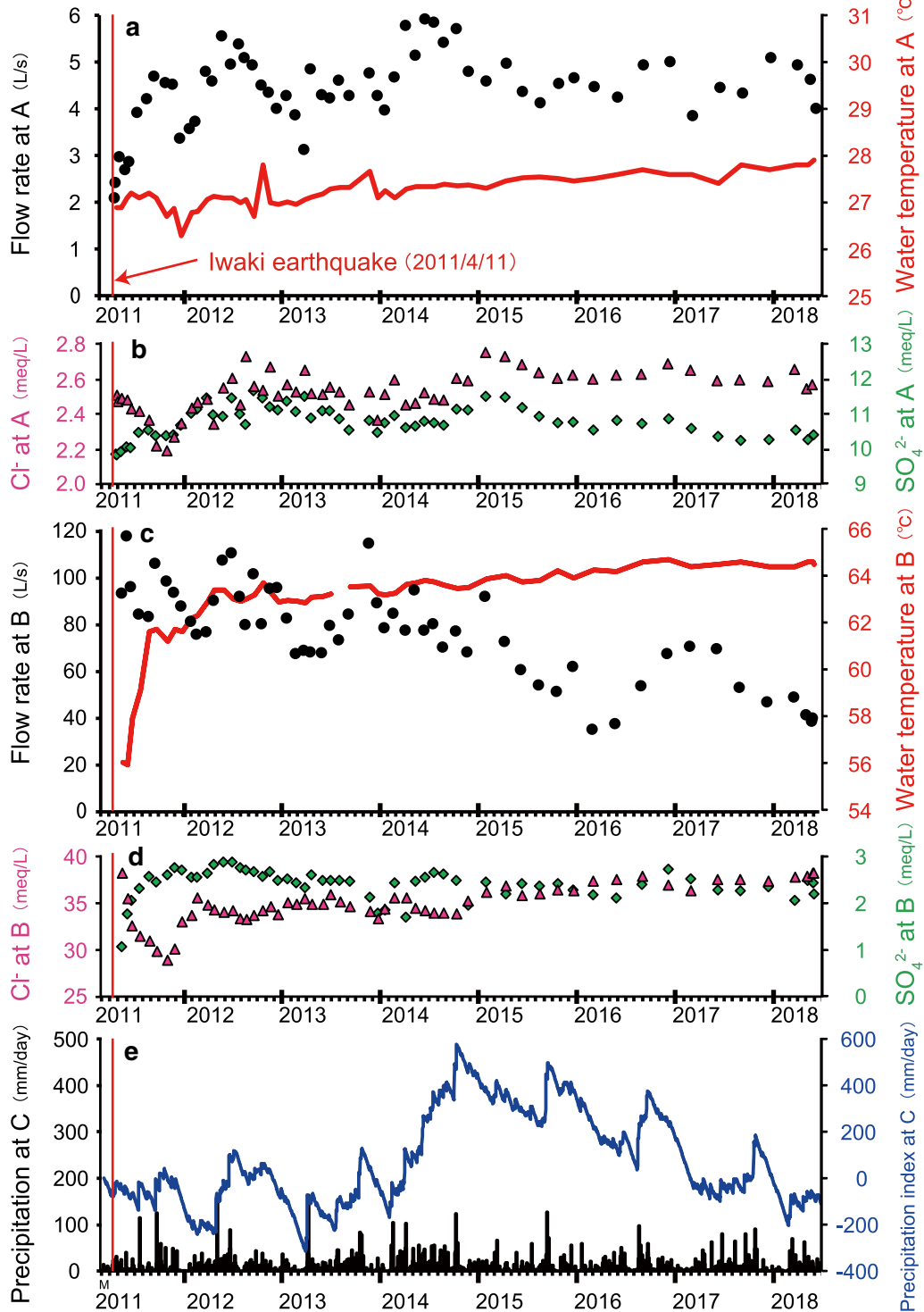
Fig. 5 Temporal variations in flow rate, temperature, and Cl$^-$ and SO$_4^{2-}$ concentrations at sites A and B (**a–d**). Precipitation data from Japan Meteorological Agency (2019), where blue line (**e**) shows precipitation index calculated by subtracting integrated value of average daily precipitation from accumulated daily precipitation

Sato *et al. Earth, Planets and Space*   (2020) 72:54

Page 9 of 11
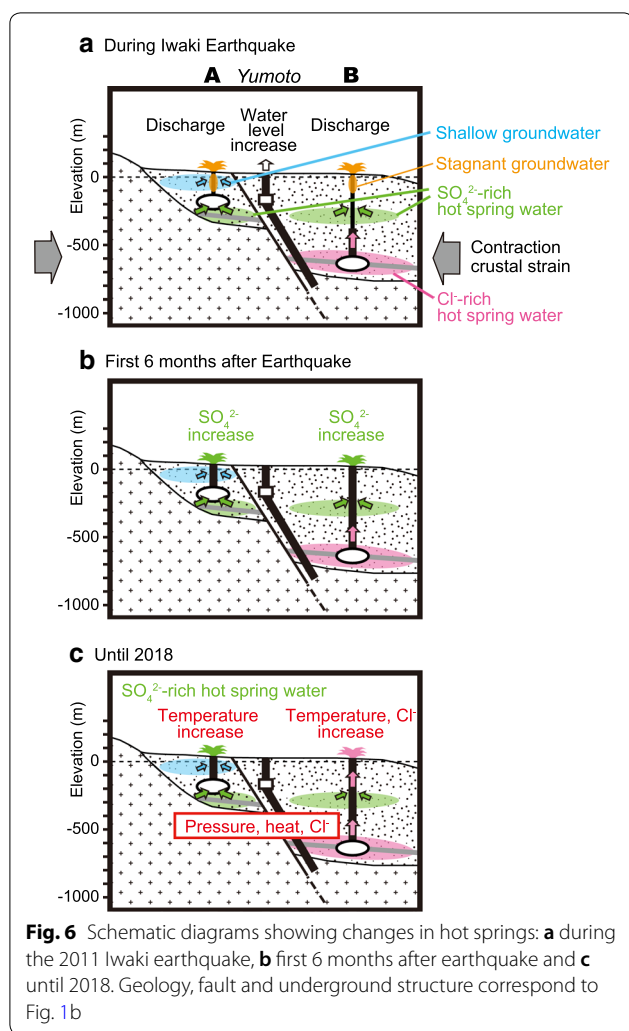
Fig. 6 Schematic diagrams showing changes in hot springs: **a** during the 2011 Iwaki earthquake, **b** first 6 months after earthquake and **c** until 2018. Geology, fault and underground structure correspond to Fig. 1b

SO_4^{2-} concentration gradually decreased and remained constant (2.3 meq/L) within a range of ± 0.2 meq/L after 2015.

During the first 6 months after the earthquake, a simultaneous increase in SO_4^{2-} and a decrease in Cl^- concentration were observed in site B (Fig. 5d); similar phenomena were observed in site A. Thus, the same model was used to explain the phenomena in both sites (Fig. 6a, b). However, unlike in site A, an inverse correlation was observed for temporal changes in the Cl^- and SO_4^{2-} concentrations in hot spring water since 2012 in site B. This inverse correlation could be attributed to rising Cl^--rich hot spring water from a depth of 600 m in site B (Fig. 6c). Based on Fig. 3, we discussed the possibility that the hot spring water at site B formed due to mixing between deep hot spring water that was discharged in the coal mine beneath site B and the shallower groundwater. This shallower groundwater was likely SO_4^{2-}-rich

groundwater, similar to the hot spring water at site A (with reference to the mixing line denoted by the thick dotted line in Fig. 3). This was consistent with changes in the inverse correlation between the Cl^- and SO_4^{2-} concentrations from long-term observations (Fig. 5d).

By comparing Fig. 5d and Fig. 5e, we observe that the SO_4^{2-} concentration increased with an increasing precipitation index. Based on the discussion above, this implied that the mixing ratio of SO_4^{2-}-rich groundwater increased as the pressure in the shallow groundwater aquifer rose with increasing precipitation. On the other hand, the increase in the Cl^- concentration reflected an increase in the mixing ratio of deep hot spring water. Therefore, observations of long-term increases in the temperature and Cl^- concentration that occurred simultaneously may indicate an increase in the mixing ratio of deep hot spring water.

Causes of continual hot spring water discharge

Since the Iwaki earthquake, hot spring water discharges at sites A and B continued for more than 7 years. In other non-volcanic areas, such long-term hot spring discharge triggered by earthquakes is rare. The reason for the hot spring continuing discharge is suggested to be a high-pressure hot spring reservoir existing in deeper regions (Fig. 1b), which formed a connection with shallower aquifers as a result of the Iwaki earthquake. We describe the evidence for the existence of such high-pressure hot spring reservoirs below.

In the Iwaki area, hot spring water discharged onto the ground surface around Yumoto before 1905 (Nakamura 1909). Therefore, a high-pressure hot spring reservoir existed beneath Yumoto at least before 1905. As previously noted, Togo et al. (2014) suggested that the origin of the hot spring water is plate boundary dehydration occurring at a depth of 50 km. In addition, the regional geothermal gradient is high in the Iwaki area (9 °C/100 m; Nakamura and Ando 1953); it is more than twice as high as the average value along the Pacific coast of the Tohoku region (4 °C/100 m; Tanaka et al. 2004). This further supports the hypothesis that thermal fluid was continuously supplied from a substantial depth.

Comparing the temporal changes in the flow rates at sites A and B, we found that the flow rate at site B has decreased since 2015. However, the flow rate at site A has not changed. This may be explained by the following two causes: (1) the rise of thermal water from the substantially deep part and (2) permeability change.

Regarding the first cause, the increase in water temperature at site B appears to have stopped since 2017 (Fig. 5c); thus, the influence of the rise of deeper thermal water may have been gradually mitigated by the discharge of large amounts of hot spring water. In contrast,

Sato *et al. Earth, Planets and Space*   (2020) 72:54

Page 10 of 11

as the water temperature continued to rise at site A, the effect of rising thermal water is likewise expected to continue, which may affect the continuation of the discharge.

On the other hand, no change in the permeability at site A and reduction in that at site B can also explain no change in the flow rate at site A and decrease in that at site B after 2015, respectively. The reduction might seem to be due to a longer channel at site B than that at site A. However, this hypothesis cannot explain the change in concentrations of Cl^- and SO_4^{2-} occurring at site A after 2013 (Fig. 5).

Conclusions

We conducted a spatial and temporal survey of the changes in hot springs generated at Iwaki in relation to the 2011 Iwaki earthquake. The conclusions are as follows:

1. The spatial distribution of the changes in the hot spring water head was clarified by surveys taken immediately after the earthquake. These survey results were compared with the spatial distribution of the changes in crustal volumetric strain calculated using a fault model. Accordingly, the model predicted contractional crustal strain in the area where we observed a rise in water head. The model further predicted an increased crustal volumetric strain in the area where we observed a drop in water head. Therefore, we suggest that changes in the crustal volumetric strain due to the earthquake caused the changes in the hot spring water level immediately after the 2011 Iwaki earthquake.

2. Long-term periodic surveys were conducted at two hot springs (sites A and B) characterized by discharge after the earthquake. Hot spring water discharge continued for over 7 years, which is rare and valuable observation in a non-volcanic area. Furthermore, we observed a slight rise in the water temperature (0.1 °C/year at site A and 0.36 °C/year at site B) and an increase in the Cl^- concentration at site B (0.4 meq/L/year).

3. Based on major anion composition analysis, we found that the hot spring water at site A had a similar composition ratio to that of the old coal mine beneath site A. Similarly, the composition ratio of hot spring water at site B was similar to that of the old coal mine beneath site B. Therefore, we suggest that hot spring water that has discharged into the coal mine flowed to the surface while mixing with shallow groundwater.

4. A possible high-pressure reservoir with hydrothermal fluids exists 40 km beneath the Iwaki area based on several pieces of evidence: the conditions of hot spring discharge before coal mining developed in the Iwaki area, the higher geothermal gradient, and results based on radiogenic iodine isotopic ratios and seismic tomography. One of the causes for the continuation of the hot spring discharge for over 7 years may be the rise of thermal water from the substantially deep part. In addition, another possible cause is the permeability change along the hot spring channels.

Authors' contributions
TS and KK carried out the field survey, hot spring water collection, flow rate and water temperature measurements, and drafted the manuscript. NM carried out the calculation of coseismic crustal strain distribution. MT carried out the chemical and isotopic analysis of hot spring water. All authors read and approved the final manuscript.

References
Arakawa T (1961) On the mine water in the Joban Iwaki coal mine. J Mining Metallurgical Inst Jpn 77(875):333–340 **(in Japanese with English abstract)**
Fukushima Y, Takada Y, Hashimoto M (2013) Complex ruptures of the 11 April 2011 Mw6.6 Iwaki earthquake triggered by the 11 March 2011 Mw9.0 Tohoku earthquake, Japan. Bull Seismol Soc Am 103:1572–1583
Geospatial Information Authority of Japan (2011) Crustal movements in the Tohoku district. Rep Coordinat Committ Earthq Predict Jpn 86:184–272

Sato *et al. Earth, Planets and Space* (2020) 72:54

Page 11 of 11

Geospatial Information Authority of Japan (2019) https://www.gsi.go.jp/. Accessed 9 May 2019

Giammanco S, Palano M, Scaltrito A, Scarfì L, Sortino F (2008) Possible role of fluid overpressure in the generation of earthquake swarms in active tectonic areas: the case of the Peloritani Mts. (Sicily, Italy). J Volcanol Geotherm Res 178:795–806

Hosono T, Hartmann J, Louvat P, Amann T, Washington KE, West AJ, Okamura K, Böttcher ME, Gaillardet J (2018) Earthquake-induced structural deformations enhance long-term solute fluxes from active volcanic systems. Sci Rep 8(1):14809. https://doi.org/10.1038/s41598-018-32735-1

Japan Meteorological Agency (2019) https://www.jma.go.jp/jma/. Accessed 7 May 2019

Kobayashi T, Tobita M, Koarai M, Okatani T, Suzuki A, Noguchi Y, Yamanaka M, Miyahara B (2012) InSAR-derived crustal deformation and fault models of normal faulting earthquake (Mj 7.0) in the Fukushima-Hamadori area. Earth Planets Space 64:1209–1221. https://doi.org/10.5047/eps.2012.08.015

Koizumi N, Kinoshita C (2017) Postseismic well water level increases at the Dogo hot spring in Japan. J Seismol Soc Jpn 70:125–134 **(in Japanese with English abstract)**

Manga M, Rowland JC (2009) Response of alum rock springs to the October 30, 2007 alum rock earthquake and implications for the origin of increased discharge after earthquakes. Geofluids 9:237–250

Manga M, Wang C-Y (2015) Earthquake hydrology. Treatise on geophysics, 2nd edn. Elsevier, Oxford, pp 305–328

Mizoguchi K, Uehara S-I, Ueta K (2012) Surface fault ruptures and slip distributions of the Mw 6.6 11 April 2011 Hamadori, Fukushima Prefecture, Northeast Japan, Earthquake. Bull Seismol Soc Am 102:1949–1956. https://doi.org/10.1785/0120110308

Muto D, Ueno H, Tamaribuchi K, Iwakiri K (2014) Characteristics and factors of the earthquakes around the northern Ibaraki Prefecture and the coastal area of Fukushima Prefecture after the 2011 off the Pacific coast of Tohoku Earthquake. Q J Seismol 78:1–28 **(in Japanese with English abstract)**

Naito H, Yoshikawa S (1999) A program to assist crustal deformation analysis. J Seismol Soc Jpn 52:101–103 **(in Japanese)**

Nakamura S (1909) Survey report on Yumoto hot spring in Iwaki district, Fukushima prefecture. Bull Geol Surv Jpn 14:35–56 **(in Japanese)**

Nakamura H (1959) Study on thermal mine water in Joban coal field. J Geol Soc Jpn 65(769):582–594 **(in Japanese with English abstract)**

Nakamura K (1971) A lesson from the Matsushiro earthquake swarm. Kagaku Asahi 10:127–133 **(in Japanese)**

Nakamura H, Ando T (1953) On the thermal water in the Joban coal field. Bull Geol Surv Jpn 4(6):355–382 **(in Japanese with English abstract)**

Nishio Y, Okamura K, Tanimizu M, Ishikawa T, Sano Y (2010) Lithium and strontium isotopic systematics of waters around Ontake volcano, Japan: implications for deep-seated fluids and earthquake swarms. Earth Planet Sci Lett 297:567–576

Ohara K (1996) Study on the mechanisms making the deep groundwater quality (part 2). JNC 400:2005–2078 **(in Japanese with English abstract)**

Okada Y (1992) Internal deformation due to shear and tensile faults in a half-space. Bull Seism Soc Am 82:1018–1040

Okada T, Yoshida K, Ueki S, Nakajima J, Uchida N, Matsuzawa T, Umino N, Hasegawa A, Group for the aftershock observations of the 2011 off the Pacific coast of Tohoku Earthquake (2011) Shallow inland earthquakes in NE Japan possibly triggered by the 2011 off the Pacific coast of Tohoku Earthquake. Earth Planets Space 63:749–754

Oki Y, Xu H, Ishizaka N, Kawauchi K (1999) Geopressured hydrothermal system associated with active faults and historical destructive earthquakes in the Shinano river seismic zone. J Jpn Soc Hot Spring Sci 48:163–181 **(in Japanese with English abstract)**

Okuyama Y, Funatsu T, Fujii T, Takamoto N, Tosha T (2016) Mid-crustal fluid related to the Matsushiro earthquake swarm (1965–1967) in northern Central Japan: geochemical reproduction. Tectonophysics 679:61–72

Roberts SJ, Nunn JA, Cathles L, Cipriani FD (1996) Expulsion of abnormally pressured fluids along faults. J Geophys Res 101(B12):28231–28252

Rojstaczer S, Wolf S (1992) Permeability changes associated with large earthquakes: an example from Loma Prieta, California. Geology 20:211–214

Sato T, Sakai R, Furuya K, Kodama T (2000) Coseismic spring flow changes associated with the 1995 Kobe earthquake. Geophys Res Lett 27:1219–1221

Sibson RH, Rowland JV (2003) Stress, fluid pressure and structural permeability in seismogenic crust, North Island, New Zealand. Geophys J Int 154:584–594

Sugai K, Matsui H, Sato S, Kitagawa Y, Sasaki M, Miyashita M, Kawachi H (1957) Geological map and explanatory text of the Joban coal field. Geol Surv Jpn 1957:143 **(in Japanese with English abstract)**

Suto I, Yanagisawa Y, Ogasawara K (2005) Tertiary geology and chronostratigraphy of the Joban area and its environs, northeastern Japan. Bull Geol Surv Jpn 56:375–409 **(in Japanese with English abstract)**

Tanaka A, Yamano M, Yano Y, Sasada M (2004) Geothermal gradient and heat flow data in and around Japan (I): appraisal of heat flow from geothermal gradient data. Earth Planets Space 56:1191–1194. https://doi.org/10.1186/BF03353340

Toda S, Tsutsumi H (2013) Simultaneous reactivation of two, subparallel, inland normal faults during the Mw6.6 11 April 2011 Iwaki earthquake triggered by the Mw9.0 Tohoku-oki, Japan. Earthquake Bull Seismol Soc Am 103:1584–1602

Togo Y, Kazahaya K, Tosaki Y, Morikawa N, Matsuzaki H, Takahashi M, Sato T (2014) Groundwater, possibly originated from subducted sediments, in Joban and Hamadori areas, southern Tohoku, Japan. Earth Planets Space 66:131. https://doi.org/10.1186/1880-5981-66-131

Tong P, Zhao D, Yang D (2012) Tomography of the 2011 Iwaki earthquake (M 7.0) and Fukushima nuclear power plant area. Solid Earth 3:43–51

Wang C-Y, Manga M (2015) New streams and springs after the 2014 Nw6.0 South Napa earthquake. Nat Commun 6:7597. https://doi.org/10.1038/ncomms8597

Wang C-Y, Manga M, Dreger D, Wong A (2004a) Streamflow increase due to rupturing of hydrothermal reservoirs: evidence from the 2003 San Simeon, California. Earthquake Geopys Res Lett 31:L10502. https://doi.org/10.1029/2004GL020124.2004

Wang C-Y, Wang CH, Manga M (2004b) Coseismic release of water from mountains: evidence from the 1999 (Mw = 7.5) Chi-Chi, Taiwan, earthquake. Geology 32:769–772

Publisher's Note